MULTIPLE-MATERIAL TOPOLOGY OPTIMIZATION OF COMPLIANT MECHANISMS CREATED VIA POLYJET 3D PRINTING

Nicholas A. Meisel[1], Andrew Gaynor[2], Christopher B. Williams[1], James K. Guest[2]
[1]Design, Research, and Education for Additive Manufacturing Systems Laboratory,
Virginia Polytechnic Institute and State University
[2]Topology Optimization Group, Johns Hopkins University

ABSTRACT

Compliant mechanisms are able to transfer motion, force, and energy using a monolithic structure without discrete hinge elements. The geometric design freedoms and multi-material capability offered by the PolyJet 3D printing process enables the fabrication of compliant mechanisms with optimized topology. The inclusion of multiple materials in the topology optimization process has the potential to eliminate the narrow, weak, hinge-like sections that are often present in single-material compliant mechanisms. In this paper, the authors propose a design and fabrication process for the realization of 3-phase, multiple-material compliant mechanisms. The process is tested on a 2D compliant force inverter. Experimental and theoretical performance of the resulting 3-phase inverter is compared against a standard 2-phase design.

Keywords: Topology Optimization, PolyJet, 3D Printing, Multiple Materials, Compliant Mechanisms, Material Jetting

1. ADDITIVE MANUFACTURE OF MULTI-MATERIAL COMPLIANT MECHANISMS

Howell defines compliant mechanisms as those which utilize the deformation of flexible members to successfully transfer motion, force, and energy [1]. This is in direct contrast to traditional mechanisms that rely on movable joints in order to perform their function. Compliant mechanisms are encountered on a daily basis in the forms of binder clips, paper clips, and various compliant latches. In addition to the various man-made examples, nature also makes use of compliant mechanisms, with many living organisms displaying parts that are both strong and flexible [2]. Advantages of compliant mechanisms include part consolidation and improved mechanism robustness. However, as the design of compliant mechanisms increases in complexity, traditional manufacturing methods become infeasible. This drives the authors' overall goal of adapting additive manufacturing (AM) methods to the context of compliant mechanism design.

While there are many examples of single-material compliant mechanisms present in everyday life, man-made, multi-material compliant mechanisms are rarer. This is because, by adding additional material phases to compliant mechanisms, the manufacturing complexity of these devices increases even more. However, by developing a consistent, repeatable method for designing and manufacturing multi-material compliant mechanisms, real improvements can be seen in application. For example, Aguirre and Frecker make a strong case for the need of multi-material compliant mechanisms in the medical field [3]. By including both a stiff and flexible material phase in the design of contact-aided compliant mechanism forceps for natural orifice translumenal endoscopic surgery, the authors were able to achieve larger total jaw openings and blocked forces. This improved mechanism performance has the potential to directly impact the success of the surgery. However, Aguirre and Frecker's design was limited by their intuitive understanding of how forceps should look. As such, the question we seek to begin answering in this paper is this: how can multi-material compliant mechanisms be designed to maximize their deflection, while remaining lightweight and leveraging the capabilities of modern AM processes?

Direct 3D PolyJet printing is one of the only AM processes capable of utilizing stiff and flexible material phases within a single build, making it uniquely qualified for manufacturing complex, multi-material compliant mechanisms. Direct 3D PolyJet printing is an AM material jetting process, wherein droplets of liquid photopolymer are deposited directly onto an elevator substrate via a series of inkjet printheads [4]. As the material is deposited, two ultraviolet (UV) lamps cure the photopolymer in multiple passes. Each subsequent layer is jetted on top of the previous one. A representation of this process can be seen in Figure 1.

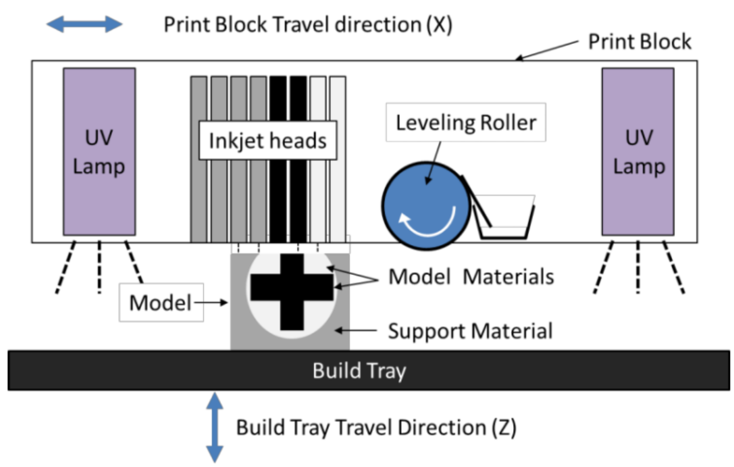

Figure 1. Representation of Direct 3D PolyJet Printing Process

The PolyJet process offers a high resolution, with a layer thickness of 16-30 microns and an in-plane resolution of 42 microns. In addition, the PolyJet process offers one significant, unique advantage among modern additive manufacturing process: the PolyJet process is capable of depositing two different materials on a pixel-by-pixel basis. One material is a rigid, white plastic-like material (VeroWhite+), while the other is an elastomeric, flexible black material (TangoBlack+). The two materials can be combined in various ratios to create nine gradient material blends with properties ranging along the continuum of the two extremes. By including multiple material phases such as these in the design of compliant mechanisms, the maximum deflection of the mechanism can potentially be improved, while simultaneously decreasing the likelihood of fatigue failure at the structure's joint-like sections.

1.1. Introduction to Compliant Mechanism Design and Topology Optimization

In general, the compliant mechanism design process can be separated into a series of key decisions that the designer must make. Each one of these decisions serves to lead the designer towards a final design methodology. The decisions include the general approach to be used (kinematics-based or optimization-based), the finite element representation of the design space (continuum, discrete, or hybrid), and the appropriate optimization algorithm (gradient-based or stochastic). A decision tree that represents these key decisions in the design process is shown in Figure 2.

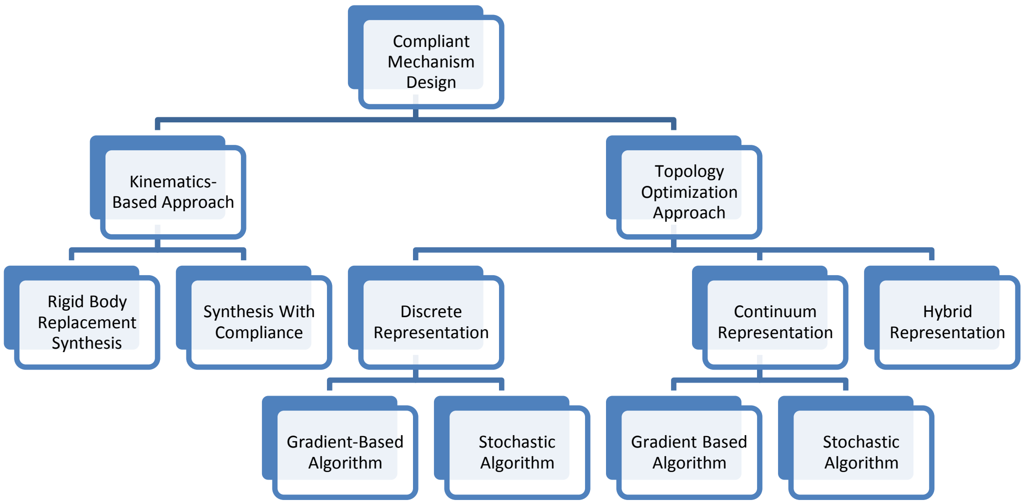

Figure 2. General Compliant Mechanism Design Decision Tree

The first decision is whether or not to pursue a kinematics based approach or a topology optimization approach. For the kinematics approach, the designer equates the desired compliant mechanism design to more traditional rigid-link kinematics design. This approach relies heavily on the designer's intuition and preconceptions regarding the final compliant system. In this way, it does not fully leverage the design freedom allowed by AM and will not be pursued herein.

For the topology optimization approach, the general compliant mechanism design domain is defined (with applied forces, supports, and desired responses) and material is systematically distributed (added or removed) from the space, according to the mathematics of a particular algorithm. This results in the effective and efficient use of material within the part. The resulting optimal design ideally satisfies all constraints while maximizing or minimizing an objective function. The use of the topology optimization approach as applied to the design of compliant mechanisms can be traced back to work by Sigmund, as well as by Frecker and coauthors [5,6].

As the next section will show, the field of topology optimization in AM is incredibly varied, with different researchers using different finite element (FE) representations and optimization algorithms according to the context of the particular problem, as well as personal preference.

1.2. Topology Optimization in Additive Manufacturing

While little to no work has yet been done regarding the manufacturing of optimized, multi-material compliant mechanisms via AM (to be discussed further in the Section 1.4), several researchers have investigated the use of AM as a means of realizing structurally optimized parts in general. The "free complexity" inherent in the AM process makes it ideal for the realization of final optimized parts. The following section seeks to elucidate the larger hubs of research in this domain.

At Loughborough University, work has been performed to assist in the design of optimized artifacts while specifically considering the necessary manufacturing constraints provided by AM.

Brackett and coauthors recently offered an overview of some of the largest perceived opportunities in this sector, including the importance of mesh resolution, the inclusion of support material constraints, as well as the adaptation of Solid Isotropic Material with Penalization (SIMP) material interpolation for lattice-based and multiple-material structures [7]. As part of this, they performed research into a method for minimizing the use of support material in optimized parts. To accomplish this, they developed a penalty function to be included with the optimization objective function, which helped to identify large downward facing edges. The penalty function helps to encourage the optimization algorithm to maintain angles that are self-supporting. In the same paper, Brackett discusses the potential for utilization of multiple-material topology optimization. He specifically mentions the abilities of the PolyJet process and offers an example of how a designer could map the various blends onto the densities produced by the SIMP. However, the author states that experiments are necessary to ensure a quality mapping scheme. Brackett also proposed a dithering-based optimization method for the creation of functionally graded lattice structures within a part [8]. Aremu and coauthors specifically investigated the SIMP and Bi-Directional Structural Optimization (BESO) approaches, comparing them and discussing their suitability when applied to AM [9]. From their investigation, they determined that adjustments should be made to both approaches in order to better arrive at complex, globally optimum solutions that might fully take advantage of the power of AM. The authors later worked towards this goal by developing a hybrid approach that combined a BESO approach with an adaptive meshing strategy, allowing for more efficient creation of fine features during optimization [10]. Watts and Hague utilized the design program "DesignLab" to investigate the performance of multiple materials in optimization. Unfortunately, the genetic algorithm approach used in their preliminary study proved too computationally expensive to efficiently optimize for multiple materials along a fine mesh. To counter this limitation, the authors proposed a variable-density unit cell library approach for optimization when considering the potential of AM [11].

At the Georgia Institute of Technology, emphasis has been placed on the development of cellular structure design, optimization, and analysis techniques for application to AM. Wang and Rosen developed a methodology for the design of conformal cellular truss structures that could easily be translated to AM parts, and later automated the design and synthesis of these structures through optimization and application to compliant structures [12–14]. Graf developed the Size Matching and Scaling (SMS) approach, which utilizes a unit cell library consisting of different truss arrangements optimized to support particular loading conditions. In addition, Graf offers a comparison of the SMS approach against the Particle Swarm Optimization method and least-squares minimization optimization method [15–17]. He found that the SMS method could offer optimized performance comparable to the results of these other two algorithms, while significantly decreasing the computation time due to the non-iterative nature of SMS. Finally, Rosen introduced a formal framework for the concept of Design for Additive Manufacturing, based on the process-structure-property-behavior framework from material science [18,19]. He demonstrated the use and applicability of this framework through the design of an optimized lattice structure to support a cover plate.

At the University of Southern California, Chen adapted Rosen's framework to assist in the design of cellular structures that offer specific compliant performance. He developed a CAD tool to design a mesostructure allowing for heterogeneous material properties within an AM printed part, in essence creating functionally graded materials from a single material [20,21]. Maheshwaraa, Bourell, and Seepersad, at the University of Texas at Austin, used ground truss optimization for investigating the use of lattice structures in the creation of deployable skins manufactured via AM [22]. At Cornell University, Hiller and Lipson have developed an automated design methodology which represents the design space as a matrix of frequency amplitude components [23,24]. These frequency components can be rendered as specific object geometry via an inverse discrete cosine transform and optimized via evolutionary algorithms. The result is less computationally expensive multi-material optimization (when compared with traditional homogenization) at the expense of feature definition (especially concerning small or sharp features). While Hiller and Lipson have not physically created their multi-material structures, they do attempt to consider the general advantages of multi-material AM.

Obviously the body of work discussed above is incredibly varied. There are researchers investigating the manufacture of optimized single-material structures in AM, researchers who are developing manufacturing rules related to single-material optimization in AM, and researchers who are investigating how multi-material optimization could generally be implemented in AM. However, in the above investigation, there were no examples of authors attempting to develop a process for the optimization and subsequent fabrication and testing of multi-material compliant mechanisms, while also incorporating the manufacturing constraints and advantages of the PolyJet printing process. It is this process that we seek to develop in our work, starting with the initial results presented herein.

1.3. Theoretical Representation of Multiple Materials in Topology Optimization

In order to apply topology optimization to the PolyJet process, an appropriate scheme for representing the multiple candidate materials must be chosen. While some potential schemes have already been touched upon in the review of AM optimization (such as Watts and Hague's use of genetic algorithms and Hiller and Lipson's frequency representation [11,23]), there are yet other multi-material representations that might also prove applicable to the realm of PolyJet printing.

One of the most well-known continuum-based topology optimization approaches is the Solid Isotropic Material with Penalization (SIMP) approach initially proposed by Bendsøe [25]. This method discretizes the design domain into a series of pixels and assigns each one a pseudo-density value. These pseudo-densities are used to interpolate between two phases of material: solid and void. In essence, if the pseudo-density value of a pixel approaches zero, it is assigned void material and if it tends towards one, it is assigned solid material. By introducing a second pseudo-density term to each pixel, it is possible to further interpolate between three material phases: one stiff, one flexible, and one void [26]. Further final material options can be added by implementing an additional pseudo-density term to each pixel in order to interpolate among each additional available material. While this method has been shown to perform reliably, it quickly becomes computationally expensive since each additional material introduces additional design variables on the order of the number of pixels in the design space (e.g. four non-zero material options creates four times as many design variables).

Another potential representation is the "barrier approach" demonstrated by Saxena [27,28]. Through this approach, he champions the use of genetic algorithms in helping to maintain the discrete nature of the available material phases, while simultaneously avoiding local minima common to the compliant mechanism optimization problem. An element density acts as the independent variable, in essence determining the elastic modulus of a particular element in relation to the elastic modulus of the stiffest candidate material. This independent elastic modulus is then used to determine which candidate material will be assigned to that particular element; if it falls below the average modulus of two neighboring materials, then the element will be assigned the material that has the lower elastic modulus of the two. Unfortunately, genetic algorithms tend to be significantly more computationally expensive than gradient-based methods, limiting their usefulness when applied to continuum-based FE representations with thousands of finite elements.

Yin and Ananthasuresh take a differing gradient-based approach in their work with multiple-material compliant mechanism analysis [29]. They use a unique peak function model to assist in material interpolation along the continuum. A normal distribution function is used to convert a continuous design problem into one with more discrete material options. As the algorithm progresses, the normal function is contracted and additional peaks begin to appear at the locations of the discrete candidate materials. The goal is to have each design variable value settle towards one of these peak values and result in a discrete final stiffness distribution. However, it is possible that intermediate stiffness values may still appear in the final result since the design variables are not necessarily driven to value at the top of the peak. Instead they are simply driven to the location where the peak has formed; any deviation from this exact peak location could result in a point that lies on the slope and thus possesses an intermediate stiffness value. The authors maintain that this formulation allows them to denote an element's material phase with only one design variable per pixel, as opposed to requiring a density variable for each potential phase. For this reason, this representation could prove beneficial as the number of candidate materials grows. However, the authors do note that the final result can depend on the initial density guess, though they use a continuation method for their model in an attempt to offset this disadvantage.

1.4. Manufacturing of Multi-Material Compliant Mechanisms

While literature has offered some discussion regarding how to optimize the design of multiple material compliant mechanisms, there has been little content detailing their actual fabrication. The few instances of literature pertaining to the fabrication of multiple material compliant mechanisms will be discussed herein, but it is important to note that none of the objects fabricated have been subjected to structural optimization. Following a review of the literature, the authors conclude that there is no prior work where multiple material compliant mechanisms have been designed, optimized, and subsequently fabricated.

One of the more prevalent examples of the manufacturing of multiple-material compliant mechanisms is from Bailey and Rajagopalan. They discuss the design and manufacture of a biomimetic leg that operates under the principle of heterogeneous material compliance [30,31]. While the final design is not driven by the concept of optimization, the authors specifically address the process of multi-material. They adapt the process of Shape Deposition Manufacturing (SDM) to allow for the creation of flexible joints while maintaining stiff members for the rest of the leg shape. SDM involves the deposition of material in layers, followed by machining in order to form the material layer into the desired shape (in this way it is like a combination of additive manufacturing and traditional CNC machining). Because the process offers continuous access to the part interior, specialized sub-pieces can be embedded during creation. In this case, the authors embedded separate flexible joints in their biomimetic leg.

Several authors have also investigated the use of multi-material molding (MMM) for the creation of multiple material compliant mechanisms [32–34]. MMM is a process whereby the various materials in the final part are created volumetrically, as opposed to the layer-by-layer methods of both AM and SDM. While there are several variations on the process, the general MMM flow involves the creation of a one material phase being molded separately and then being inserted into a mold for the second stage material phase. Filling this second stage mold will embed the first material phase within the part.

For the fabrication of small scale multiple material compliant mechanisms, there are two examples that are derivations of the MMM process. Rajkowski proposes a prototyping process that uses a curable rigid polymer as well as a curable, flexible silicone as the two material phases [35]. By placing the material phases down in bulk and using a mask to cure only the desired sections of the part, the author offers a quick, inexpensive solution for the fabrication of multiple-material mechanisms on the millimeter scale. Vogtmann proposes a process whereby the negative space for the flexible material phase is cut from a bulk piece of the rigid phase [36]. The flexible material is deposited, cured, and planed, before the desired mechanism profile is cut from the bulk material.

While the above processes have been shown to successfully create multiple material compliant mechanisms, they all also have limitations when considering complexity and distributed compliance of the final pieces. The examples presented are relatively geometrically simple when compared to traditional results of multiple-material optimization, and thus were all manufacturable. However, these processes do not scale well. As the complexity of topology and multi-material distribution increases, the processes will require significantly more user interaction and time investment to create the necessary mechanisms. In addition, the presented examples all rely on the principle of lumped compliance, where the flexible material phase is implemented at the location that would traditionally be represented by a revolute joint. These processes would be ill-prepared to manufacture mechanisms based on distributed compliance, where the flexible material phases would be more interspersed among the rigid material.

1.5. Context

The study presented in this paper demonstrates a start-to-finish process for the realization of optimized, multi-material compliant mechanisms. This represents an important first step in unlocking the design potential of the multi-material PolyJet process. The authors determine an appropriate compliant mechanism design process, based on the decision tree presented earlier in Figure 2, in Section 1.1. The peak function optimization method (Section 2.2) and a variation on the SIMP optimization method (Section 2.3) are applied to the design of a compliant force inverter, a well-known compliant mechanism case-study. Results from experimentally testing the printed multi-material optimized structures are provided in Section 3. Closure is offered in Section 4.

2. PROCESS FOR DESIGN AND MANUFACTURING OF 2D, 3-PHASE COMPLIANT MECHANISMS

This section discusses two different optimization approaches that were implemented to design optimized compliant mechanisms. Section 2.2 and Section 2.3 discuss the peak function optimization method and SIMP optimization method, respectively, and how they are applied to multiple material optimization. In addition, the section will discuss the logic behind the selection of these two approaches.

2.1. Determination of Compliant Mechanism Design Process Suitable for PolyJet Printing

As has already been mentioned in Figure 2, the design of compliant mechanisms can be divided into a hierarchal decision tree. For the first decision, we have already discussed that the use of the kinematics approach does not sufficiently leverage the potential of AM, so we instead follow a topology optimization path. The next decision is dependent on how the designer wishes to represent the finite element discretization in the design space. The discrete representation, such as that seen in the ground structure approach, has the potential to drastically reduce the computational intensity of the optimization routine, due to the lower number of finite elements in the design space. However, this comes at the cost of resolution, with the discrete representation limited in the amount of detail that it can show in the optimal topology. A continuum representation, on the other hand, offers the potential for a truer representation of the optimal topology (depending on the chosen mesh size). It is worth noting that a hybrid representation might be able to balance the speed of the discrete representation with the resolution of the continuum method. While such hybrid approaches generally exist in literature, such as a truss-continuum model for optimizing steel and concrete placement [37], the authors are unaware of any hybrid representations being used in conjunction with multiple material AM at this time. We have thus elected to eliminate a hybrid representation from consideration in this preliminary study.

The authors have instead chosen to pursue a continuum representation, due in part to the quality of its resolution as well as the way in which a continuum representation aligns with the PolyJet process' method of printing. When printing, the PolyJet process utilizes a series of multi-colored bitmaps that are sent to the printer. Each bitmap represents a single slice of the printed part, with multiple colors used in each slice to denote the material to be deposited. While the ability does not currently exist, the authors hope to eventually be able to use the image outputs from 2D topology optimization as a direct bitmap slice input to the printer. In this way, translating the topology optimization output to an STL file will become unnecessary and the process of manufacturing optimized multi-material compliant mechanisms will become more streamlined.

The final decision to be made when considering the design decision tree in Figure 2 is whether to solve the chosen formulation with a gradient-based optimization algorithm or stochastic search optimization algorithm. Stochastic algorithms, such as genetic algorithms and particle-swarm optimization, randomly sample the design space and are thus capable of handling discrete formulations and facilitating escape from low performance local minima. These types of algorithms, however, can be incredibly slow and may break down in high dimension spaces such as those of continuum topology optimization. Although strategic dimension control algorithms have been proposed for such cases (e.g., [38]), gradient-based optimization methods are much better suited to handle the many design variables inherent in a continuum representation. In this preliminary study, both the interior-point algorithm and Method of Moving Asymptotes (MMA) will be utilized.

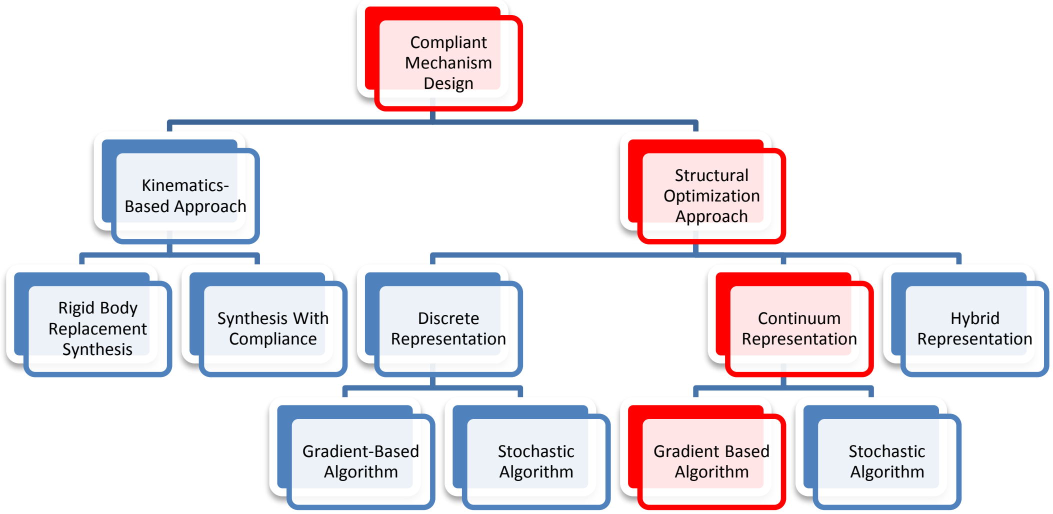

Figure 3. Chosen Compliant Mechanism Design Approach (Highlighted in Red)

2.2. Optimization Approach 1: Peak Function Method

The peak function multiple-material representation from Yin and Ananthasuresh (discussed in Section 1.3) was selected for investigation in this study, mainly because of the potential to eventually optimize for all eleven of the PolyJet process's material blends without increasing the number of design variables. In this particular approach, an interpolation function is used to directly relate the design variable of each pixel to the elastic modulus of the pixel. The interpolation function takes the following form, representative of a normal distribution function:

$$E = \sum_{m=1}^{N} E_m e^{-(\rho-\mu_m)^2/2\sigma_m^2} + E_{void} \tag{1}$$

In this interpolation, ρ is the design variable of each pixel, m is the material index, N is the total number of candidate materials, and μ_m and σ_m are the mean and standard deviation of the Gaussian distribution function for the designated candidate materials. The value of σ_m is gradually decreased as the optimization progresses. This slowly converts the interpolation from a smooth single-peaked function to a function with prominent peaks at each value of μ_m and E_{void} elsewhere.

MATLAB's built-in *fmincon* function is used to perform the actual optimization and design variable update step in the overall TO process. The interior-point algorithm is selected as the gradient-based algorithm of interest for this study. The desire is to keep the TO process as "black-box" as possible; a desire which MATLAB's *fmincon* fulfills handily. However, one of the main drawbacks of this combined *fmincon*/peak function formulation as it has been described is that it the final topology is very sensitive to a number of user-determined values, including the values of E_{void}, μ_m, and σ_m. The result is an almost trial-and-error approach to achieving reasonable convergence, which will be discussed in more detail in Section 3.1.

2.3. Optimization Approach 2: Multivariate SIMP Method

An alternative to the Peak Function Method is proposed here that uses a combination of design variables in a SIMP scheme to produce multi-material topologies. The idea is that each phase contributes to a 'total' Young's modulus for an element. The base modulus is the modulus of the most compliant phase (typically void), and each phase i has the capability of adding stiffness. For the case of equal jumps ΔE in Young's modulus between the phases, this may be written as follows:

$$E = \sum_{i=1}^{n} \rho(\phi)_i^{\eta} \Delta E \tag{2}$$

where n is the number of design variables ρ per element. To achieve a three phase solution containing voids ($E = 0$), stiff material ($E = E_{stiff}$), and complaint phase ($E = 0.5\ E_{stiff}$), two elemental design variables per element are required and $\Delta E = 0.5\ E_{stiff}$. An element is then assigned the stiff phase when $\rho_1 = \rho_2 = 1$, compliant phase when ρ_1 or ρ_2 are equal to 1, and void when $\rho_1 = \rho_2 = 0$. Parameter η is the SIMP exponent and is needed to drive the design variables to 0 or 1, and ultimately the modulus of an element, to the allowable magnitudes. Embedded in this formulation is the Heaviside Projection Method (HPM) that uses the independent design variables ϕ. These design variables are projected onto the ρ space using regularized Heaviside functions in a manner that enables direct control over the minimum length scale of designed features. This is meant to mimic the AM manufacturing process as material is computationally 'deposited' into the design domain in a circular shape with radius r_{min}, the resolution length scale of the liquid droplets [39,40]. The Method of Moving Asymptotes is used as the optimizer [41], and full algorithmic details are available in [42].

3. CASE STUDY: COMPLIANT FORCE INVERTER

In order to demonstrate the utility of the presented optimization, and printing method, the authors consider the well-established example of a compliant force inverter. This case study was initially demonstrated in [5] and has become one of the benchmarks for demonstrating compliant mechanism optimization processes. As seen in Figure 4 the design space for the mechanism is square, with the top and bottom points on the left side of the design space fixed. An input force is applied to the left hand-side of the space, along with an input spring constant value. A reaction force and spring constant are also applied to the right hand side of the space. The objective of the study is to maximize the work done on the output spring. If k_{out} is large, then the greatest force transfer to the output location is targeted. If k_{out} is small, then the greatest displacement of the output location is targeted.

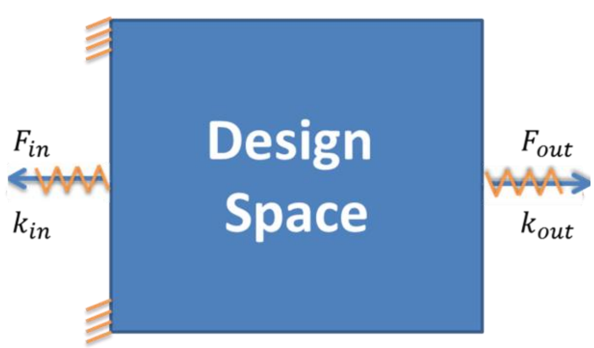

Figure 4. Design Space and Loading for Inverter Case Study

It should be noted that the analysis used in the topology optimization was limited to the linear displacement assumption. As literature has shown, at best this assumption limits the usefulness of the final topology and, at worst, renders it completely inaccurate [43,44]. However, the creation of these optimized pieces should still offer a useful point of comparison between 2-phase and 3-phase results, even though the experimental deflection values of each specimen will likely differ significantly from any predicted theoretical values.

3.1. Force Inverter – Peak Function Approach

As already discussed, there are a series of optimization parameters that must be decided on in order to achieve convergence of the *fmincon*/peak function optimization approach. Key among these are the material properties of the candidate materials, specifically the modulus of elasticity and Poisson's ratio. For this study, properties were chosen which generally represent the ratio between the moduli of our two non-void candidate printing materials. The inputs to the optimization algorithm were $E_1 = 2$ and $E_2 = 1$. This represents the 2:1 stiffness ratio between the pure VeroWhite+ printed material (at approximately 3000 MPa) and RGD8530 polypropylene-like digital material (at approximately 1500 MPa). The Poisson's ratio was assumed to be equal for the two materials. This is a necessary simplification due to the scarcity of material information regarding PolyJet materials at the moment. The void material phase was designated with $E_{void} = 0.001$. This renders the void material significantly more flexible than the most flexible non-zero material, while still maintaining a value large enough to stabilize convergence of the algorithm. Other critical optimization parameters for the three-phase peak-function study were selected as follows (attempting to select values similar to those presented by Yin and Ananthasuresh in their initial study):

Table 1. Optimization Constant Values for Peak Function Method

$2\sigma_1^2$	$2\sigma_2^2$	μ_1	μ_2	ρ_0	F_{in}	F_{out}	k_{in}	k_{out}
0.05	0.05	0	0.3	0.4	3	-3	1	0.001

Initial investigation of this approach using the compliant force inverter case study unfortunately yields less than desirable results. While the peak function method has the potential to optimize for any number of candidate materials, in practice it seems to be too highly sensitive to a number of parameters. For example the images in Figure 5 demonstrate the effect of changing the values of $2\sigma_1^2$ and $2\sigma_2^2$ on both the shape of the final topology and on the distribution of the two non-void materials throughout the structure. The mesh size for these example specimens is 80 x 40. Figure 5a shows the topology with $2\sigma_{1,2}^2 = 0.04$ and Figure 5b shows the topology with $2\sigma_{1,2}^2 = 0.05$. Note that by adjusting these values, the placement of stiff and flexible material within the design space changes significantly. In addition, the theoretical tip deflection of the structure increases decreases by approximately 7% when changing from $2\sigma_{1,2}^2 = 0.04$ to $2\sigma_{1,2}^2 = 0.05$. Adjusting the values of μ_1, μ_2, and ρ_0 likewise yield significant changes in the final topology and material distribution.

(a) (b)

Figure 5. Final Topology Results when a) $2\sigma_{1,2}^2 = 0.04$ and b) $2\sigma_{1,2}^2 = 0.05$ (Grey = Flexible Material, Black = Stiff Material)

In addition, although the peaks used in the interpolation method will tend to centralize the non-zero elements about the peak, there does not appear to be any motivation for the algorithm to drive any particular element to the candidate material stiffness located at the top of the peak. Instead, it is possible for a location along the peak's slope to be selected, which could result in regions that are not fully assigned to either the stiff or flexible phase.

Since there does not appear to be any methodology for the selection of the $2\sigma_1^2, 2\sigma_2^2, \mu_1, \mu_2$, and $\rho_0$terms, attempts at convergence become dependent on trial and error. This is unsuitable for the field of AM, since this trial and error approach would need to be duplicated for each unique set of boundary conditions. When the "mass customization" of AM allows for a variety of different parts (and thus boundary conditions) in a single build tray, a more robust optimization method is required. As such, the authors direct their attention to the traditional SIMP approach and offer a variation on the approach that better accommodates the use of multiple materials.

3.2. Force Inverter – Multivariate SIMP Approach

The compliant inverter is now solved using the multivariate SIMP approach with the same parameter values given Section 3.1. The multivariate approach uses nine node quad elements instead of the traditional four node quads. This is done to help eliminate the occurrences of one-node hinges in the final topology. As mentioned previously, this SIMP approach uses MMA and resulting in a very efficient optimization algorithm. This allows for the use of fine mesh (120 x 60 and utilizing symmetry), which produces a smooth final topology. With a 30% volume fraction, the following solution is attained:

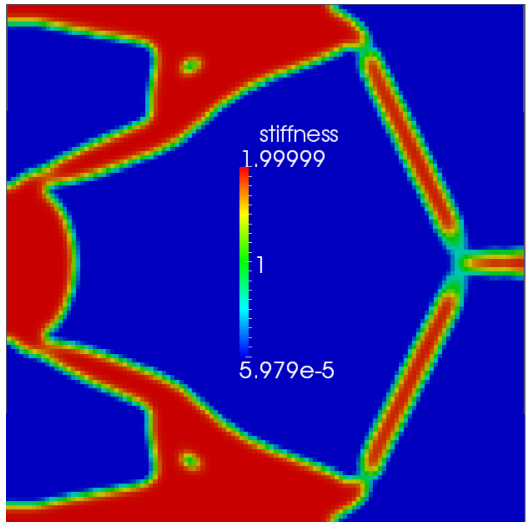

Figure 6. 3-Phase Inverter Result from Multivariate SIMP Approach

These preliminary results align with intuition - the algorithm places the stiff phase in the truss-like pieces and the compliant phase in the joints. Also promising is the elimination of one-node hinges by use of nine node quadrilateral elements. However, this comes at additional computational expense.

The same optimization parameters are used with the multivariate SIMP approach to design a traditional 2-phase force inverter (with one non-zero candidate material and void). This enables the authors to evaluate and compare the performance offered by additional candidate materials in topology optimization. The optimized 2-phase inverter is shown in Figure 7.

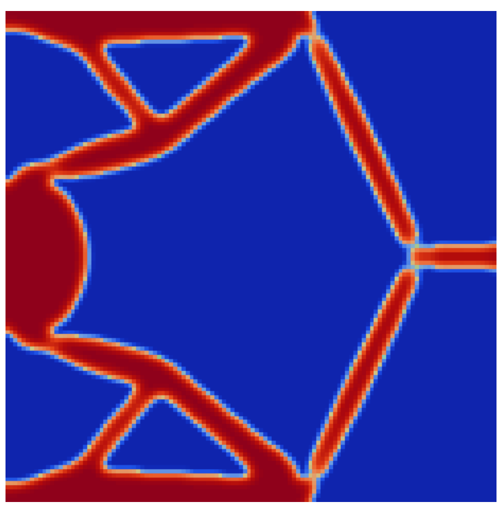

Figure 7. 2-Phase Inverter Result from Multivariate SIMP Approach

Both the 2-phase and 3-phase inverters were printed on an Objet Connex 350. The stiff material was VeroWhite+ and the flexible material was RGD8530. Each inverter was printed to fill a 12.7 x 12.7 cm bounding box, with a thickness of 3.56 mm. An additional structure was added to each compliant mechanism in order to provide a location for the necessary force to be applied, as well as to ensure a cantilevered fixation at the appropriate point on the structure. The final printed specimens can be seen in Figure 8.

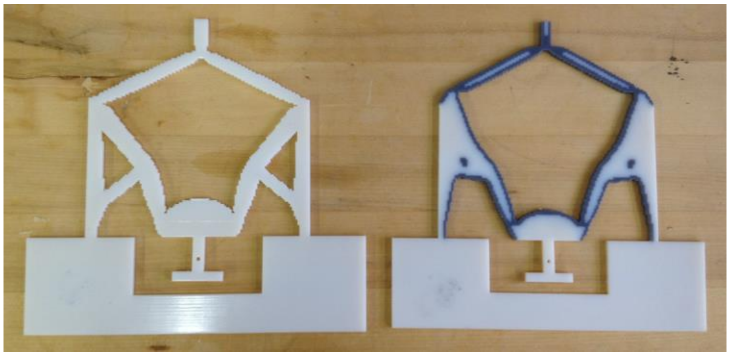

Figure 8. Compliant Specimens with Load and Cantilever Attachments

Each inverter was actuated by applying a 9.1 kg load at the "T" shaped attachment at the bottom of mechanism. The output tip location was marked before and after application of the load. The resulting mechanism motion is shown in Figure 9. The 2-phase inverter tip deflected 2.20 mm while the 3-phase inverter deflected 9.98 mm, a performance improvement of 453%.

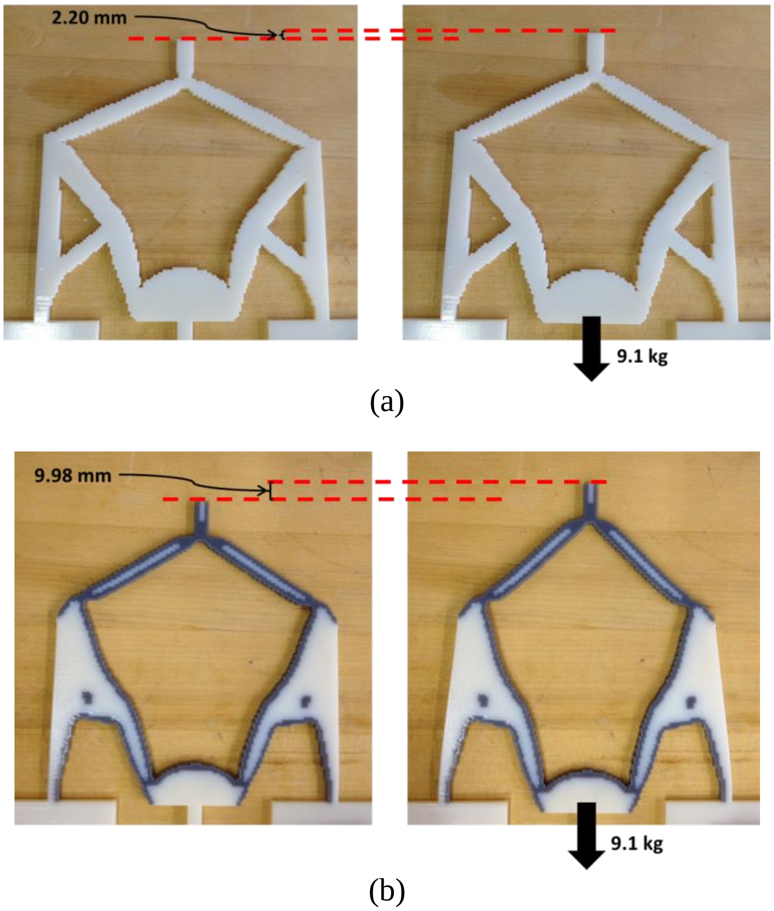

Figure 9. Deflection of a) 2-Phase Inverter and b) 3-Phase Inverter (both under 9.1 kg applied load)

To demonstrate the ultimate potential of the PolyJet process's array of materials, the flexible material in the 3-phase inverter was changed with TangoBlack+, the most elastomeric material offered by the Objet process. It is important to note that this substitution has not been optimized at this time; the ratio of VeroWhite+ to TangoBlack+ stiffness is closer to 20:1, instead of the 2:1 ratio the optimization was performed for. However, it nevertheless demonstrates the dramatic displacement improvements that might be achieved in time. The TangoBlack+ and VeroWhite+ inverter achieved a deflection of 10.98 mm with only 540 g of applied load, as shown in Figure 10.

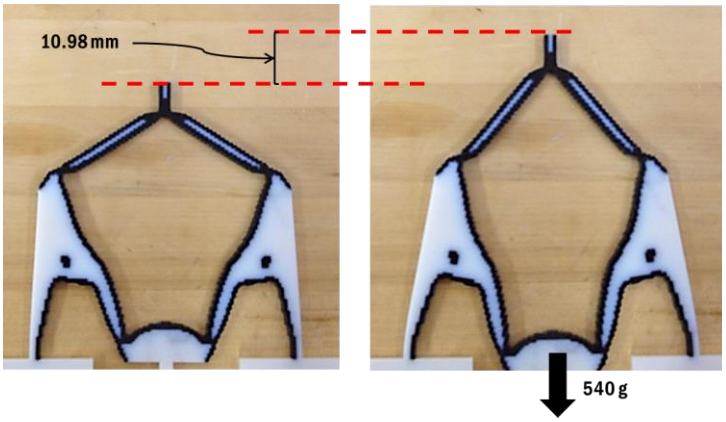

Figure 10. Deflection of 3-Phase Inverter with TangoBlack+ Material (under 540 g of applied load)

4. CONCLUSIONS AND RECOMMENDATIONS FOR FUTURE WORK

In this paper, the authors have presented a preliminary study into the development of a start-to-finish process for the design and manufacture of optimized, multi-material compliant mechanisms. The previous literature was reviewed in order to determine an appropriate compliant mechanism design and optimization approach, taking care to consider the unique opportunities afforded by multi-material PolyJet printing. While the peak function approach seemed initially promising due to its ability to handle all of the PolyJet's material blends without increasing the number of design variables, the trial and error approach necessary to achieve convergence limits its usefulness in AM application. A more robust multivariate SIMP approach was thus proposed to provide better results to the multi-material topology optimization problem. Experimental results of the compliant force inverter problem show that the addition of a second non-zero candidate material increases the deflection of the compliant inverter from 2.20 mm to 9.98 mm.

Future work will first focus on optimizing the inverter structure for use with the elastomeric TangoBlack+ material. Second, additional candidate materials will be introduced into the optimization routine to create optimized inverters with more material phases. Research will also be performed into automatically smoothing the boundaries of each material phase, to remove any undesirable stress concentrations that may be present because of the pixelated nature of the final printed specimen. Finally, efforts will be placed on quantifying the material properties and printing limitations of the PolyJet process, so that manufacturing limitations might be included in the topology optimization algorithm.

5. REFERENCES

[1] Howell L. L., 2001, Compliant Mechanisms, Wiley.
[2] Vogel S., 1995, “Better Bent Than Broken,” Discover, (May), pp. 62–67.
[3] Aguirre M. E., and Frecker M., 2010, “Design and optimization of hybrid compliant narrow-gauge surgical forceps,” ASME 2010 Conference on Smart Materials, Adaptive Structures and Intelligent Systems, American Society of Mechanical Engineers, Department of Mechanical and Nuclear Engineering, Pennslyvania State University, University Park, PA, United States, pp. 779–788.
[4] Stratasys, 2013, “Objet 350 Connex: Build Mid-Size Prototypes in Multiple Materials” [Online]. Available: http://stratasys.com/3d-printers/design-series/precision/objet-connex350.
[5] Sigmund O., 1997, “On the Design of Compliant Mechanisms Using Topology Optimization,” Mechanics of Structures and Machines, **25**(4), pp. 493–524.
[6] Frecker M. I., Ananthasuresh G. K., Nishiwaki S., Kikuchi N., and Kota S., 1997, “Topological Synthesis of Compliant Mechanisms Using Multi-Criteria Optimization,” Journal of Mechanical Design, Transactions of the ASME, **119**(2), pp. 238–245.
[7] Brackett D., Ashcroft I., and Hague R., 2011, “Topology Optimization for Additive Manufacturing,” 22nd Annual International Solid Freeform Fabrication Symposium, pp. 348–362.
[8] Brackett D., Ashcroft I., and Hague R., 2011, “A Dithering Based Method to Generate Variable Volume Lattice Cells for Additive Manufacturing,” 22nd Annual International Solid Freeform Fabrication Symposium, pp. 671–679.
[9] Aremu A., Ashcroft I., Hague R., Wildman R., and Tuck C., 2010, “Suitability of SIMP and BESO Topology Optimization Algorithms for Additive Manufacture,” 21st Annual International Solid Freeform Fabrication Symposium, pp. 679–692.
[10] Aremu A., Ashcroft I., Wildman R., Hague R., Tuck C., and Brackett D., 2011, “A Hybrid Algorithm for Topology Optimization of Additive Manufactured Structures,” 22nd Annual International Solid Freeform Fabrication Symposium, pp. 279–289.
[11] Watts D. M., and Hague R., 2006, “Exploiting the Design Freedom of RM,” 17th Annual International Solid Freeform Fabrication Symposium, pp. 656–667.
[12] Wang H. V., and Rosen D. W., 2001, “Computer-Aided Design Methods for the Additive Fabrication of Truss Structures,” Georgia Institute of Technology.
[13] Wang H. V., and Rosen D. W., 2006, “An Automated Design Synthesis Method for Compliant Mechanisms with Application to Morphing Wings,” ASME Mechanisms and Robotics Conference, pp. 1–9.
[14] Wang H. V., Chen Y., and Rosen D. W., 2005, “A Hybrid Geometric Modeling Method for Large Scale Conformal Cellular Structures,” ASME Computers and Information in Engineering Conference, pp. 421–427.
[15] Graf G. C., 2009, “Development of Specialized Base Primatives for Meso-Scale Conforming Truss Structures,” Georgia Institute of Technology.
[16] Graf G. C., Chu J., Engelbrecht S., and Rosen D. W., 2009, “Synthesis Methods for Lightweight Lattice Structures,” ASME 2009 International Design Engineering Technical Conferences and Computers and Information in Engineering Conference, ASME, pp. 579–589.

[17] Chu J., Engelbrecht S., Graf G., and Rosen D. W., 2010, “A Comparison of Synthesis Methods for Cellular Structures with Application to Additive Manufacturing,” Rapid Prototyping Journal, **16**(4), pp. 459–472.

[18] Rosen D. W., 2007, “Computer-Aided Design for Additive Manufacturing of Cellular Structures,” Computer-Aided Design and Applications, **4**(5), pp. 585–594.

[19] Chu C., Graf G., and Rosen D. W., 2008, “Design for Additive Manufacturing of Cellular Structures,” Computer-Aided Design and Applications, **5**(5), pp. 686–696.

[20] Chen Y., and Wang S., 2008, “Computer-aided product design with performance-tailored mesostructures,” Computer-Aided Design and Applications, **5**(1-4), pp. 1–11.

[21] Li Y., Chen Y., and Zhou C., 2009, “Design of Flexible Skin for Target Displacements Based on Meso-Structures,” Proceedings of the ASME 2009 International Design Engineering Technical Conferences, pp. 1–14.

[22] Maheshwaraa U., Bourell D., and Seepersad C. C., 2007, “Design and Freeform Fabrication of Deployable Structures with Lattice Skins,” Rapid Prototyping Journal, **13**(4), pp. 213–225.

[23] Hiller J. D., and Lipson H., 2009, “Multi material topological optimization of structures and mechanisms,” 11th Annual Conference on Genetic and Evolutionary Computation, pp. 1521–1528.

[24] Hiller J. D., and Lipson H., 2009, “Design Automation for Multi-Material Printing,” 20th Annual International Solid Freeform Fabrication Symposium, pp. 279–287.

[25] Bendsøe M. P., 1989, “Optimal shape design as a material distribution problem,” Structural optimization, **1**(4), pp. 193–202.

[26] Bendsøe M., and Sigmund O., 1999, “Material Interpolation Schemes in Topology Optimization,” Archive of Applied Mechanics, **69**, pp. 635–654.

[27] Saxena A., 2005, “Topology Design of Large Displacement Compliant Mechanisms with Multiple Materials and Multiple Output Ports,” Structural and Multidisciplinary Optimization, **30**(6), pp. 477–490.

[28] Saxena A., 2002, “On Multiple-Material Optimal Compliant Topologies: Discrete Variable Parameterization Using Genetic Algorithm,” ASME 2002 International Design Engineering Technical Conferences and Computers and Information in Engineering Conference, pp. 1–12.

[29] Yin L., and Ananthasuresh G. K., 2001, “Topology Optimization of Compliant Mechanisms with Multiple Materials Using a Peak Function Material Interpolation Scheme,” Structural and Multidisciplinary Optimization, **23**, pp. 49–62.

[30] Bailey S. A., Cham J. G., Cutkosky M. R., and Full R. J., 1999, “Biomimetic Robotic Mechanisms via Shape Deposition Manufacturing,” Robotics Research: The 9th International Symposium, pp. 403–410.

[31] Rajagopalan S., Goldman R., Shin K.-H., Kumar V., Cutkosky M., and Dutta D., 2001, “Representation of heterogeneous objects during design, processing and freeform-fabrication,” Materials & Design, **22**(3), pp. 185–197.

[32] Bejgerowski W., Gerdes J. W., Gupta S. K., and Bruck H. A., 2011, “Design and Fabrication of Miniature Compliant Hinges for Multi-Material Compliant Mechanisms,” The International Journal of Advanced Manufacturing Technology, **57**(5-8), pp. 437–452.

[33] Bejgerowski W., Gerdes J. W., Gupta S. K., Bruck H. A., and Wilkerson S., 2010, “Design and Fabrication of a Multi-Material Compliant Flapping Wing Drive Mechanism for Miniature Air Vehicles,” ASME 2010 International Design Engineering Technical

Conferences and Computers and Information in Engineering Conference, ASME, pp. 69–80.

[34] Gouker R. M., Gupta S. K., Bruck H. A., and Holzschuh T., 2006, "Manufacturing of Multi-Material Compliant Mechanisms Using Multi-Material Molding," International Journal of Advanced Manufacturing Technology, **30**, pp. 1049–1075.

[35] Rajkowski J. E., Gerratt A. P., Schaler E. W., and Bergbreiter S., 2009, "A multi-material milli-robot prototyping process," 2009 IEEE/RSJ International Conference on Intelligent Robots and Systems, IEEE Computer Society, Mechanical Engineering Department, Institute for Systems Research, University of Maryland, College Park, MD 20742, United States, pp. 2777–2782.

[36] Vogtmann D. E., Gupta S. K., and Bergbreiter S., 2011, "A Systematic Approach to Designing Multi-Material Miniature Compliant Mechanisms," ASME 2011 International Design Engineering Technical Conferences and Computers and Information in Engineering Conference, ASME, pp. 211–221.

[37] Gaynor A., Guest J., and Moen C., 2012, "Reinforced Concrete Force Visualization and Design Using Bilinear Truss-Continuum Topology Optimization," Journal of Structural Engineering, **139**(4), pp. 607–618.

[38] Guest J. K., and Smith Genut L. C., 2010, "Reducing Dimensionality in Topology Optimization Using Adaptive Design Variable Fields," International Journal for Numerical Methods in Engineering, **81**(8), pp. 1019–1045.

[39] Guest J. K., Prévost J. H., and Belytschko T., 2004, "Achieving Minimum Length Scale in Topology Optimization Using Nodal Design Variables and Projection Functions," International Journal for Numerical Methods in Engineering, **61**(2), pp. 238–254.

[40] Guest J. K., 2009, "Topology Optimization with Multiple Phase Projection," Computer Methods in Applied Mechanics and Engineering, **199**(1–4), pp. 123–135.

[41] Svanberg K., 1987, "The Method of Moving Asymptotes—a New Method for Structural Optimization," International Journal for Numerical Methods in Engineering, **24**(2), pp. 359–373.

[42] Guest J. K., Asadpoure A., and Ha S.-H., 2011, "Eliminating Beta-Continuation from Heaviside Projection and Density Filter Algorithms," Structural and Multidisciplinary Optimization, **44**(4), pp. 443–453.

[43] Buhl T., Pedersen C., and Sigmund O., 2000, "Stiffness Design of Geometrically Nonlinear Structures Using Topology Optimization," Structural and Multidisciplinary Optimization, **19**, pp. 93–104.

[44] Bruns T. E., and Tortorelli D. A., 2001, "Topology Optimization of Non-Linear Elastic Structures and Compliant Mechanisms," Computer Methods in Applied Mechanics and Engineering, **190**(26–27), pp. 3443–3459.